High-Accuracy, Unsupervised Annotation of Seismocardiogram Traces for Heart Rate Monitoring

Federico Cocconcelli, Niccolò Mora, Guido Matrella, and Paolo Ciampolini

***Abstract*— This article presents an unsupervised, automated procedure for the analysis of Seismocardiogram (SCG) signals. SCG is a measure of chest vibrations, induced by the mechanical activity of the heart, which allows extracting relevant parameters, including heart rate (HR) and HR variability (HRV). An initial self-calibration is performed, solely based on the SCG traces, yielding a suitable heartbeat template (personalized for each subject). Then, beat detection and timing annotation are performed in two steps: at first, candidate beats are identified and validated, by means of suitably defined detection signals; then, precise timing annotation is achieved by best aligning such candidate beats to the previously extracted template. The algorithm has been validated on two separate data sets, featuring different acquisition setups: the first one is the publicly available Combined measurement of ECG, Breathing and Seismocardiogram (CEBS) database, reporting SCG signals from the subjects lying in supine position, whereas the second one was acquired using a custom setup, involving the sitting subjects. Results show good sensitivity and precision scores (98.5% and 98.6% for the CEBS database, and 99.1% and 97.9% for the Custom one, respectively). In addition, comparison with electrocardiogram (ECG) gold-standard is given, showing good agreement between the beat-to-beat intervals computed from SCG and the ECG gold-standard: on average, R^2 scores of 99.3% and 98.4% are achieved on the CEBS and Custom data sets, respectively. Furthermore, a low rms error is achieved on the CEBS and Custom data sets, amounting to 4.6 and 6.2 ms, respectively (i.e., 2.3 T_s and 3.1 T_s, where T_s is the sampling period): such results are well compared with related literature. Validation on two different data sets indicates the robustness of the proposed methodology.**

***Index Terms*— Accelerometer, active assisted living (AAL), heart rate (HR), microelectromechanical system (MEMS), Seismocardiogram (SCG), vital sign monitoring.**

I. Introduction

ADVANCEMENTS in the information and communication technology (ICT) and the Internet of Things (IoT) technology are driving innovation in many different fields, by allowing more devices to interact in a seamless way. Active assisted living (AAL) [1] and, in general, smart environments are positively impacted by the emerging IoT paradigm: traditional systems are being redesigned to support native interaction in interconnected environments. With IoT devices making their way into the AAL realm, a wealth of information becomes available, covering different aspects. For example, information from multiple sensor was analyzed and fused together to detect the fall events or suspicious inactivity periods [2] in the homes of frail users. Moreover, indirect information about a person's general wellbeing was extracted from the presence and motion sensors in home environments [3]: anomalies or deviations (either sharp or abrupt) in habits and routines can be quantitatively assessed, potentially suggesting the underlying health issues. Such an approach is, for instance, being adopted to complement the medical protocols for persons recovering from stroke events in [4]. In such a context, indirect assessment of health and wellbeing status by means of behavioral analysis fosters care continuity.

In general, fusing information coming from many sources and different domains enhances the potential of the AAL monitoring systems. In particular, fusion among behavioral and physiological data may result in more comprehensive and detailed pictures, greatly supporting caregiving insightfulness and allowing developing new services. Suitable devices are needed, though, with low intrusiveness and low cost features, which are essential to AAL monitoring. Among most relevant physiological indicators, heart activity plays a relevant role in health assessment: information such as heart rate (HR) and HR variability (HRV) can be easily extracted by means of wearable sensors that analyze the electrocardiogram (ECG) [5] or photoplethysmogram (PPG) [6] signals. This article focuses on a different technique for gathering such information, introduced by Salerno and Zanetti [7] and based on the study of vibrational patterns related to the mechanical activity of the heart. Indeed, recent advancements in the low-power microelectromechanical system (MEMS) technology opened up to the possibility of deploying low-cost wearable devices for acquiring acceleration patterns directly from the chest surface: the study of such information is the object of Seismocardiogram (SCG) [8], [9]. As sketched in Fig. 1, relevant cardiac events are clearly detectable in the SCG, including aortic valve opening (AO)/aortic valve closure (AC) and mitral valve opening (MO)/mitral valve closure (MC) and isovolumic movement (IM). An ECG is shown in the

Manuscript received September 3, 2019; revised December 19, 2019; accepted January 3, 2020. Date of publication January 17, 2020; date of current version August 11, 2020. The Associate Editor coordinating the review process was Roberto Ferrero. *(Corresponding author: Federico Cocconcelli.)*

The authors are with the Dipartimento di Ingegneria e Architettura, Università degli Studi di Parma, 43121 Parma, Italy (e-mail: federico.cocconcelli@unipr.it; niccolo.mora@unipr.it; guido.matrella@unipr.it; paolo.ciampolini@unipr.it).

Color versions of one or more of the figures in this article are available online at http://ieeexplore.ieee.org.

Digital Object Identifier 10.1109/TIM.2020.2967135

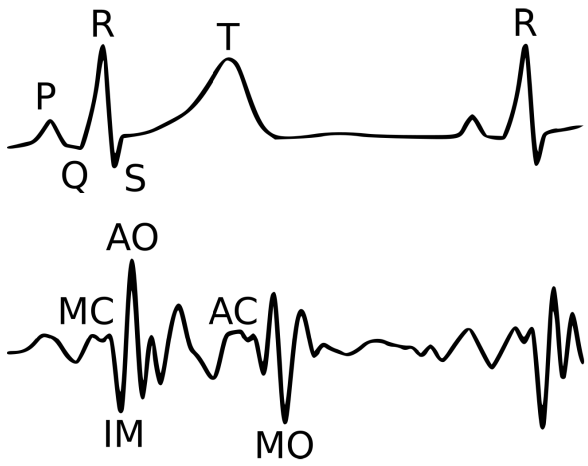

Fig. 1. Typical SCG patterns, temporally related with the electrical activity of the heart measured by an ECG.

figure as well, allowing relating the mechanical and electrical descriptions, representing the heart cycle. Although different waveforms are exhibited, SCG provides comparable HR information (focusing on the heart mechanical activity) with the previously mentioned techniques. The SCG technique is particularly appealing for AAL environment, being less intrusive than ECG and being suitable for convenient embedding (e.g., in smart clothes). Furthermore, the combination of SCG and ECG/PPG opens up to the evaluation of new parameters of interest (as mentioned later).

This article is framed into the more general picture of the AAL monitoring systems, where information is gathered from many different sources. The proposed methodology can be applied in the continuous HR and HRV monitoring scenarios, requiring no skin contact (neither electrodes nor photoemitters/detectors). Furthermore, the chest sensor inherently carries much further relevant information, related to the user motion, balance, and posture. This provides valuable context to the heart activity indicators, that is, the same sensor can be used to track the quality and quantity of physical activity (e.g., walking), with SCG analysis being carried out when artifacts are less present (e.g., during the rest phases). In a more general sense, the SCG outcomes could be fused with further behavioral information coming from the AAL monitoring system, possibly resulting in a more accurate and deeper insight.

With the inclusion of such a new dimension in the monitoring scheme, constraints in terms of costs and intrusiveness have to be met: this article presents an automatic procedure for analyzing the SCG traces in a fully unsupervised way, allowing detecting heartbeats and its characteristic patterns precisely, focusing on still subjects. Beat detection and localization are carried out in a self-consistent way, without requiring ECG-based calibration. Each phase aims at optimizing different performance figures (sensitivity/precision in the detection and beat-to-beat time accuracy in the localization case), exploiting derived signals that have been explicitly devised and introduced. Effectiveness of the approach is progressively assessed by means of statistical testing, discussing the impact of each phase on overall performance. With respect to previous findings in [10], the current approach improves in three ways.

1) In previous work, initial calibration required the acquisition of a reference ECG trace. In the current approach, such ECG-assisted calibration phase is no longer needed.
2) The methods are validated on two distinct data sets: a) the Combined measurement of ECG, Breathing and Seismocardiogram (CEBS) database, publicly available at the PhysioBank repository [11] and b) a custom-collected data set, acquired by means of a low-cost, embedded hardware setup, which relates more closely to the practical uses in AAL contexts. The proposed methodology is, therefore, validated on two different acquisition setups and experimental protocols.
3) The achieved performance is significantly improved, and it is also positively compared with other related literature. Overall, an average of 98.5% and 99.1% sensitivity scores is achieved for the CEBS and Custom databases, respectively, whereas precision were found to be 98.6% and 97.9%. In addition, a low rms error is achieved on the CEBS and Custom data sets, amounting to 4.6 and 6.2 ms, respectively (i.e., 2.3 T_s and 3.1 T_s, where T_s is the sampling period).

The rest of this article is organized as follows. Section II briefly reviews the related works and introduces the methodologies, discussing the details ranging from data set features to algorithm implementation. Section III presents the achieved results, statistically evaluating the impact of the main algorithm's steps and parameters on the overall performance. In the same section, relevance of the results is discussed, by comparing with previous works, also discussing inherent implications and limitations. Finally, Section IV draws the conclusions.

II. Methods

A. Related Work

As mentioned, SCG is the study of chest vibrations induced by the mechanical activity of the heart. Such a waveform results from many factors indeed [12], including cardiac contractions, mitral and aortic valve dynamics, and blood flow turbulence. Vibrations are most commonly measured by means of 3-axial MEMS accelerometers [13] or 6-degrees of freedom inertial measurement units (IMUs), which add rotational speed to the information being recorded [14]. It is worth mentioning that, besides accelerometry, other SCG measurement techniques exist in literature. For example, by using an airborne pulse-Doppler ultrasound system, HR was successfully estimated on the clothed skin [15]; other works make contactless measurements of HR using radar systems tuned at different frequency bands [16], [17], laser-Doppler vibrometry [18], [19], microwave sensors [20], and video-based analysis [21]. However, such solutions require bulky equipment and are not suited for daily use, in the AAL-oriented scenario that this article is aiming at. In the following, therefore, only the accelerometer approach is considered.

SCG waveforms can be acquired at different positions on a subject's chest wall. The most common place is over the

sternum, and the measurement device is typically held in place by a medical tape or textile supports [22]. Nonetheless, many works explore different sensor placements, attempting to maximize the sensitivity to specific cardiac phases (e.g., mechanical dynamics of a specific heart valve) [23]. Indeed, a possible application of SCG is to provide appropriate timing reference to compute the intervals that relate the mechanical and electrical activities of the heart: fusing information from ECG, it is possible to compute parameters like the preejection period (PEP, i.e., the interval between the electrical depolarization of the left ventricle and the beginning of ventricular ejection) or left ventricular ejection time (LVET, i.e., the period of blood flow across the aortic valve) [24].

Acquiring an SCG can be challenging in motion contexts: artifacts (e.g., from walking) contaminate the physiological signal, making annotation less precise. In order to reduce such an effect, many techniques were developed in literature. For example, Jain and Tiwari [25] propose to reduce walking-induced artifacts by detecting the time intervals of possible footsteps (using the head-to-toe acceleration component), discarding SCG information near them. Instead, Javaid *et al.* [26] attempt to compute PEP intervals from moving subjects by making a combined use of the ECG and SCG traces: an empirical mode decomposition (EMD)-based method is used for denoising SCG waveforms, achieving a correlation coefficient r between 0.75 and 0.86, depending on the walking speed, with respect to the chosen reference (namely, impedance cardiography); in this case, however, identification of heartbeat is guided by simultaneous analysis of ECG. Similarly, an independent component analysis (ICA) method is proposed to separate noise from the SCG signals and compute the PEP intervals in [27] statistically. Finally, a normalized least mean square (NLMS) adaptive filter is presented in [28]: by using a delayed version of the signal as noise term, narrowband interference is reduced. However, an ensemble-average approach is taken to estimate the mean HR, since single beat-to-beat interval computation is too noisy: this can jeopardize the calculations of parameters like HRV. In the following, methods will be presented aiming at maximizing consistency in beat-to-beat interval annotation, possibly assuming quasi-static, quiet conditions. This article aims at a specific application target, consisting in monitoring seniors users and their daily living patterns in a continuous fashion: within this scenario, significant time intervals during which the assumption of quasi-quiescence should be reasonable are to be expected, indeed, allowing to provide the AAL system with frequent and reliable assessment of heart parameters, to be integrated into behavioral patterns analysis.

B. Data Sets and Preprocessing

As stated in Section I, the proposed methodology was tested on two different data sets. The first one is the CEBS database [29], publicly available online and suitable for benchmarking with other works. It contains records of 20 users, whose ECG, SCG, and breath signals were simultaneously sampled while lying in the supine position (the measurements refer to the dorsoventral axis, perpendicular to the chest).

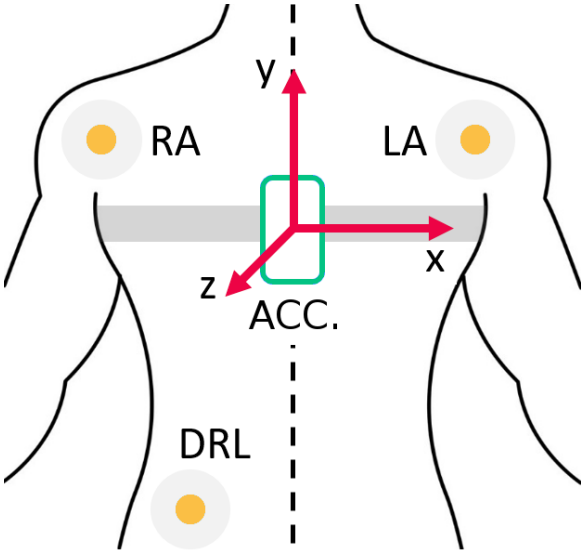

Fig. 2. Measurement setup: left arm (LA) and right arm (RA) form the modified Lead-I ECG, whereas the driven right leg (DRL) electrode reduces common-mode noise; the accelerometer's reference system is also reported.

This data set features almost 50 min of data per user, allowing validating methods in the medium time span; more details on this database can be found online at the project Web site on PhysioNet [11].

The second data set, instead, was recorded for this article, exploiting low-cost custom hardware, suitable for deployment in the AAL scenarios. The records consist of relatively shorter acquisitions (about 4 min each), during which ECG and SCG were sampled, with subjects comfortably resting on a chair. In order to compare consistently to the CEBS database, the same acceleration axis is monitored, i.e., the one perpendicular to the chest (z-axis in Fig. 2). Overall, 13 healthy subjects (nine males and four women, age 35.2 ± 16.0) were recruited on a volunteering base, following the guidelines of the Helsinki declaration on ethical principles. In the experimental protocol, the SCG was acquired by means of a triaxial accelerometer device (ADXL355 by Analog Devices Inc., Norwood, MA, USA) placed over the subject's sternum, held in place by a light chest strap. In order to achieve a proper signal quality, particular care was taken to ensure a firm placement of the sensor: this required a tight-fitting chest strap and, if needed, the use of filling material on the sensor, to better adapt to different body shapes. Simultaneously, for performance assessment purpose only, an ECG was acquired using a modified Lead-I setup: signals were taken from the left and right shoulders using disposable Ag/AgCl electrodes, amplified by a dedicated integrated circuit (AD8232, Analog Devices Inc.); a third electrode was used, placed on the right limb, in order to drive the patient potential so that common-mode noise from the mains is reduced. The combined SCG/ECG experimental setup is shown in Fig. 2, which also reports the orientation system of the accelerometer. Signals were recorded at a sampling frequency of 500 Hz by means of an Advanced RISC Machine (ARM) Cortex M0 (Arm Holdings, Cambridge, England, U.K.). Data are wirelessly

streamed (IEEE 802.11b/g/n) by means of the Transmission Control Protocol (TCP)/IP protocol. A Python environment, running on a standard desktop PC, was used for data gathering, storing, and analysis.

Preprocessing steps were applied before signal analysis. In particular, the CEBS database signals were downsampled from the original 5-kHz sampling frequency by a factor of 10, to match the other data set acquisition rate. Data were filtered by suitably designed finite-impulse response (FIR) filters, with a (2−14)-Hz passband for the SCG trace and (1−30) Hz for the ECG signal, providing a minimum 40-dB attenuation in the stopbands. As the last preprocessing step, data were scaled by means of z-scoring

$$x_{\mathrm{SCG}} = \frac{x - \mu_x}{\sigma_x} \tag{1}$$

where x is the signal of interest, μ_x is its mean, and σ_x its standard deviation.

C. Data Analysis

An SCG heartbeat pattern consists of several peaks and valleys, which may differ in amplitude and duration depending on the unique physiological/anatomical characteristics of each subject. In addition, due to slight unavoidable body movements, the SCG signal can contain spurious peaks and valleys, not related to heart activity. Due to such inherent noise, a preliminary phase is introduced, instead of simply searching for given peaks. Candidate beats are detected according to signal energy variations, at a local level; to do so, the following detection signal x_{DET} is introduced:

$$x_{\mathrm{DET}}[n] = \sum_{k=0}^{M-1} b[k] \cdot x_{\mathrm{SCG}}^2[n-k] \tag{2}$$

where x_{SCG} is the preprocessed SCG signal and $b[k]$, $k = 0, \ldots, M-1$ are the coefficients of a low-pass FIR filter: in this article, $M = 256$ and the cutoff frequency is 2 Hz. In order to isolate better the actual signal from high-variance noise, the x_{DET} signal is further processed by means of a sliding-window binary filter, defined as follows:

$$x_{\mathrm{SQR}}(i) = \begin{cases} 1, & \text{if } x_{\mathrm{DET}}(i) \geq \mu_{i:i-p} + k \cdot \sigma_{i:i-p} \\ -1, & \text{otherwise} \end{cases} \tag{3}$$

where $\mu_{i:i-p}$ is the average computed over the last p points ($p = 30$ in this article), $\sigma_{i:i-p}$ the sample standard deviation, and k is a multiplication factor that regulates how much the sample needs to stand out against the computed window statistics. Too low values of k imply that more peaks are discovered, possibly including the spurious ones; on the other hand, too high values of k might skip potential heartbeats. Such a parameter was empirically calibrated, yielding a value of $k = 2$, suitable for detecting most heartbeats for different subjects and data sets. Positive values of x_{SQR} indicate time intervals suitable for including heartbeat locations. The block diagram in Fig. 3 illustrates the processing sequence used to obtain x_{DET} and x_{SQR}.

The candidates extracted from x_{SQR} are then inspected: simple, short rebounds are just filtered out, whereas too long or too short beat-to-beat intervals are removed by constraining the HR range to a practical one (e.g., 40–180 beats/min) and by imposing the relative maximum difference between the consecutive beats. In order to search for the missed beats in a given interval, the k parameter in (3) is lowered, and search is performed again.

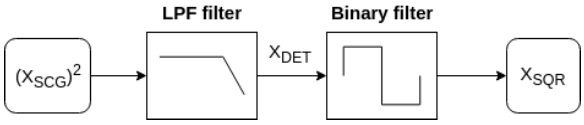

Fig. 3. Block diagram representing the sequence of operations adopted to obtain the signals x_{DET} and x_{SQR}.

Once detected, validated candidates can then be used for calibration purposes: an ensemble is formed from the identified candidates (this article considers $n_{\mathrm{ENS}} = 20$ sample traces in the ensemble). However, in order to extract a template from the ensemble, individual beats need first to be realigned: positive intervals in x_{SQR}, in fact, just coarsely define beat location, and their durations are not necessarily uniform. A sliding approach is adopted to this purpose: at first, two candidate periods are centered; then, a cross correlation metric is maximized, in order to fine-tune the alignment. The extent of possible delays τ_S to maximize such a metric is chosen such that

$$\tau_S = s \cdot \sigma_{\mathrm{SQR}} \tag{4}$$

where σ_{SQR} represents the standard deviation of the identified positive-x_{SQR} intervals' length and s is a multiplicative coefficient whose impact will be discussed in the results. Restricting the set of the cross correlation delays to $\pm\tau_S$ reduces the risk of misalignment and better adapts to individual subjects. Once the samples of the ensemble are aligned, a template $x_{\mathrm{SCG},T}$ is extracted by taking the median of such waveforms. It is worth remarking that such a calibration procedure is performed in a completely unsupervised way, without any involvement of the ECG signal.

The SCG annotation phase follows the same process used for template definition. Candidates are first identified and refined among the positive intervals in x_{SQR}; then, precise time instants are marked by maximizing the cross correlation between the extracted template and the SCG traces in such intervals. All the methodology's steps are summarized as the pseudocode in Algorithm 1.

III. Results and Discussion

It is worth remarking here that the purpose of the present method is not to diagnose heart diseases, for which specific medical devices are better suited; instead, the aimed target includes relatively healthy senior persons, whose activities are to be continuously monitored in the context of smart AAL systems: precise HR and HRV indicators can effectively enhance the insightfulness of a behavioral analysis framework. Thus, we leave major arrhythmias out of the method's scope, assuming a regular heart rhythm to be monitored. Under such an assumption, it is possible to compare the performance of the proposed methodology against the ECG reference (i.e., the absence of ectopic beats or rhythm disturbances

Algorithm 1 Detection of Heartbeat Events

Inputs:

- x_{SCG}: SCG signal

Begin:

- Compute x_{DET} and x_{SQR} according to eq. (2) and (3), respectively
- *Calibration*:
  - Validate positive x_{SQR} intervals ($40 \div 180$ bpm + maximum relative increase/decrease)
  - Compute τ_S from eq. (4)
  - Incrementally align sample beats from positive x_{SQR} intervals by means of cross correlation over centers $\pm\, \tau_S$
  - Extract SCG beat template (median)
- *Annotation*:
  - Validate positive x_{SQR} intervals
  - Around candidates, find the delay τ that maximally aligns x_{SCG} to template $x_{\mathrm{SCG},P}$ ($|\tau| \leq \tau_S$)
  - Mark the corresponding time instant as heartbeat

Return index of possible heartbeats

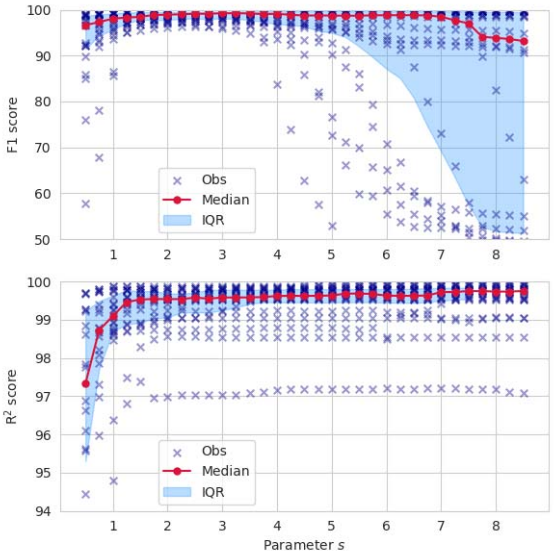

Fig. 4. Variation of F1 (top) and R^2 (bottom) scores with respect to the s parameter. Shaded area represents the interquartile range, solid lines the median, whereas crosses represent individual performance.

in the examined records allows to correlate precisely the electrical and mechanical activities of the heart). In particular, performance will be evaluated in terms of ability to detect heartbeats and to localize them precisely in time. The former ability implies detecting as much beats as possible, without causing false detections; the latter quantifies the errors in SCG beat-to-beat intervals, with respect to the ECG-derived ones. To perform such benchmarking, R peaks are identified in the ECG traces by detecting the QRS complexes: this can be accomplished by the validated and well-known Pan–Tompkins algorithm [30]. Such R peaks are assumed as ground truth for beat-to-beat interval times. IM/AO complexes in the SCG (referring to Fig. 1) are selected as target for the detection and annotation phases: SCG-derived beat-to-beat intervals are defined accordingly. However, the delay between the R peaks and IM/AO complexes varies from person to person. In order to assess detection performance, such delays were manually estimated on a per-subject basis, identifying their mean value: this provides a reference about the expected location of the complex, in the case of correct detection. It is worth underlying that this manual annotation was carried out with the benchmarking purposes only and it is not used in any phase of the actual methodology.

Detection of an SCG heartbeat is considered successful [true positive (TP)] if it falls within a window of 100 ms from this expected value. On the other hand, a missed beat between two R peaks is classified as false negative (FN); finally, a beat outside the specified tolerance window and between two R peaks is considered as a false positive (FP). Based on these definitions, the following metrics are introduced.

1) *Sensitivity* (or *TP Rate*), i.e., percentage of correctly identified reference points: Sens = TP/(TP + FN).
2) *Precision*, i.e., percentage of TP in all detected points: Prec = TP/(TP + FP).
3) *F1 Score*, i.e., the harmonic mean of precision and sensitivity: $\mathrm{F1} = 2(\mathrm{Prec} \cdot \mathrm{Sens})/(\mathrm{Prec} + \mathrm{Sens})$.

Furthermore, in order to assess the agreement between the ECG and SCG-derived beat-to-beat intervals, it is useful to define the estimated interval errors as

$$e_i = t_{\mathrm{RR},i} - t_{\mathrm{CC},i} \tag{5}$$

where $t_{\mathrm{RR},i} = t_{R,i} - t_{R,i-1}$ is the ith R-R interval and $t_{\mathrm{CC},i} = t_{\mathrm{SCG},i} - t_{\mathrm{SCG},i-1}$ is the time interval between two SCG Complexes (C-C). For convenience, let us define t_{RR} and t_{CC} as the time series of the matched $t_{\mathrm{RR},i}$ and $t_{\mathrm{CC},i}$ intervals.

The following performance metrics are then used.

1) Error mean (μ_e) and standard deviation (σ_e).
2) Root-mean-squared error (RMSE)

$$\mathrm{RMSE} = \sqrt{\frac{1}{N}\sum_{i=0}^{N-1} e_i^2} \tag{6}$$

where N is the number of beat-to-beat intervals.

3) Coefficient of determination (or R^2)

$$R^2 = \left[\frac{\mathrm{cov}(t_{\mathrm{RR}}, t_{\mathrm{CC}})}{\sigma_{\mathrm{RR}} \cdot \sigma_{\mathrm{CC}}}\right]^2 \tag{7}$$

where σ_{RR} and σ_{CC} are the standard deviations of t_{RR} and t_{CC}, respectively.

In Sections III-A–III-C, results are presented as follows: first, the impact of the x_{SQR} signal, the second-pass refinements, and the τ_S parameter on the performance metrics are analyzed; then, the overall scores are presented on both data sets; finally, such results are discussed and compared with current related literature.

A. Incremental Performance Assessment

As discussed before, beat detection and annotation are the two separate tasks: for the former one, a detection signal

was introduced in (2), with the purpose of highlighting the high-energy portions of the SCG signal, where beats are likely to be found. However, as described in Section II-C, not all x_{DET} peaks are directly related to heartbeats: the x_{SQR} signal in (3) was introduced with the purpose of better highlighting candidate heartbeat locations. In order to prove the effectiveness of this further processing step, statistical analyses were carried out, using the CEBS database (since it provides a larger basis of both users and heartbeats). In particular, the performance in coarse beat detection was compared under two different conditions: namely, by directly setting an optimal threshold on the x_{DET} signal (i.e., a unique threshold on x_{DET} that maximizes the *a posteriori* performance) or by using the x_{SQR} signal as a guide. In both cases, no second-pass refinements on anomalous beat-to beat intervals were performed, comparing just the raw effect of simple thresholding versus x_{SQR} signal. Results show that the precision score is significantly better in the latter case: on average, an improvement from 92.2% to 98.8% is observed; such a difference is also statistically meaningful ($p < 0.01$), as pointed out by a Wilcoxon signed-rank test on the individual subjects' scores. No statistically significant difference was noted in terms of sensitivity: from those considerations, we can conclude that the x_{SQR} signal helps indeed in reducing FPs without affecting the FNs.

In order to boost the sensitivity, a second-pass refinement is performed on the candidate beats extracted from x_{SQR}, as previously discussed; a comparison between not performing versus performing such second-pass refinement shows that an average increase of approximately 3% is achieved, in terms of sensitivity, in the latter case. Such an improvement is also statistically significant ($p < 0.01$), as pointed out by a Wilcoxon signed-rank test, as above.

The tests performed so far demonstrate the effectiveness of the main beat detection steps in the proposed methodology. Thus, keeping this part of the algorithm fixed, the impact of the annotation phase on the detection performance is studied as follows. Recall from (4) that a maximum span was defined, over which alignment between a candidate beat and the template is performed: if waveforms are not correctly aligned, annotation is less precise. It is, therefore, relevant, investigating how changes in τ_S [in particular, changes in parameter s of (4)] affect the F1 and R^2 scores, i.e., both the beat detection and localization effectiveness, respectively. In fact, small values of parameter s may limit the extent of possible delays, resulting in poor alignment; on the other hand, too large values increase the chance of spurious peak detection and correlations. Fig. 4 summarizes such experiments, performed on the wider CEBS database, for $s \in [0.5 - 8.5]$: solid line represents the median score across all subjects (whose individual performances are reported as scattered crosses), whereas the shaded areas depict the interquartile range (i.e., the [25th − 75th] percentile range). As anticipated, F1 metric is sensitive to the s parameter value: a decreasing trend is present for the increasing values of such parameter, also indicated by the larger interquartile range and the wider scattering of individual performance. On the other hand, the R^2 metric is less affected by higher values of s parameter: this is partly because FP and FN beats (which affect the F1 metric) are not considered in the matched ECG and SCG intervals; nonetheless, lower values of s do not allow proper exploration of the SCG signal and annotation is, therefore, less precise (resulting in lower R^2 scores). It can be noted that a practical range of s exists, around 3.25, that maximizes the F1 score while preserving the R^2 metric: values approach 98.5% and 99.3%, respectively.

TABLE I
SCORES ACHIEVED ON THE CEBS DATA SET

Record ID	Sensitivity [%]	Precision [%]	R^2 [%]
1	95.7	95.6	99.2
2	99.4	99.4	99.8
3	98.0	97.5	98.7
4	98.8	98.6	99.7
5	97.8	97.6	99.5
6	97.7	97.4	99.8
7	99.7	99.6	98.5
8	99.6	99.8	99.7
9	99.2	99.0	99.9
10	98.9	98.8	97.3
11	97.3	98.7	99.1
12	98.1	99.2	99.0
13	99.7	99.7	99.6
14	97.1	96.8	99.6
15	99.7	99.7	98.7
16	99.8	99.8	99.6
17	99.0	99.0	99.5
18	96.5	97.0	99.8
19	99.4	99.3	99.5
20	99.4	99.4	99.8
Mean	98.5	98.6	99.3
Std	1.2	1.2	00.6

B. Overall Performance Analysis

After analyzing the impact of different algorithm phases, we may now assess overall performance: by considering both CEBS and Custom data sets, a more comprehensive test is performed, considering different scenarios and evaluating the robustness of the proposed methodology with respect to differences in setups (supine versus standing position; different data acquisition instruments). It is worth further underlining that calibration is fully self-consistent, with beat detection and annotation of SCG traces being carried out in a completely unsupervised way, that is, ECG is introduced here for benchmarking purposes only and does not contribute to calibration at all.

Tables I and II show the performance figures achieved on the CEBS and Custom data sets, respectively. On average, good performance is achieved in all reported metrics. In particular, a high average sensitivity is achieved in both data sets (98.5% and 99.1% for the CEBS and Custom data sets, respectively), proving good capability to detect as much heartbeats as possible; at the same time, the precision is high (98.5% and 99.1% for the CEBS and Custom data sets, respectively), demonstrating the detection capability, without being too prone to FPs. Bearing in mind the limitation of differently sized data sets (approximately 50 min of records per subject for the CEBS data set and 4 for the Custom one), statistical analysis of achieved scores was conducted to find the differences between the two: a Mann–Whitney U-test was used

TABLE II
SCORES ACHIEVED ON THE CUSTOM DATA SET

Record Id	Sensitivity [%]	Precision [%]	R^2 [%]
1	100.0	97.2	99.3
2	100.0	100.0	98.5
3	100.0	99.1	99.2
4	96.5	96.5	97.6
5	100.0	100.0	97.9
6	100.0	100.0	97.4
7	97.0	96.2	97.3
8	100.0	99.1	99.5
9	100.0	100.0	99.7
10	100.0	100.0	99.4
11	95.0	84.1	96.5
12	100.0	100.0	98.9
13	100.0	100.0	98.6
Mean	99.1	97.9	98.4
Std	1.7	4.2	1.0

for the purpose. According to such a test, the observed slight difference in sensitivity (in favor of the Custom data set) is indeed significant, from a statistical point of view ($p \approx 0.01$); no difference was found, instead, in terms of precision.

High R^2 scores were achieved in both data sets (99.3% and 98.4% for the CEBS and Custom databases, respectively): this indicates that good agreement is obtained between the ECG- and SCG-derived beat-to-beat intervals. The slight difference in favor of the CEBS data set is, indeed, significant, according to the statistical test as above. Such a difference may be partially due to the difference in the data set size: if more points are gathered, errors tend to have less impact on the overall score; nonetheless, we report such finding for completeness' sake. Further insights about ECG and SCG correlation is given by the Bland–Altman plots in Fig. 5: each scatter plot shows the relation between the average and the difference in t_{RR} and t_{CC}, for both CEBS and Custom data sets [Fig. 5(a) and (b), respectively]. Ideal behavior should result in points scattered along the horizontal $t_{\mathrm{RR}} - t_{\mathrm{CC}} = 0$ line. Points deviating from that trend imply measurement errors: their RMSE value is reported (red dashed lines), together with $\pm 2\sigma_e$ (blue dotted line), whereas the average error, representing systematic bias, is shown as a black solid line. Overall, an rms error as low as 4.6 ms was achieved on the CEBS data set, whereas for the Custom one, the RMSE figure is approximately 6.2 ms: in terms of sampling interval $T_s = 2$ ms, such scores are 2.3 T_s and 3.1 T_s, respectively. The $\pm 2\sigma_e$ uncertainty intervals are ± 9.2 ms (i.e., 4.6 T_s) for the CEBS data set, ± 12.4 ms (i.e., 6.2 T_s) for the Custom one. As observed for the R^2 score, the CEBS data set statistically tends to perform better; however, the actual RMSE difference between the two data sets is just slightly less than one sampling interval (0.8 T_s). Furthermore, the experimental setup involved in the Custom data set is slightly more prone to motion artifacts, given both the upright sitting position and the less firm mechanical coupling between the accelerometer and the subjects' body. Overall, the achieved results prove good robustness of the proposed methodology, with respect to different measurement setups.

Concerning future deployment in AAL context, power consumption is relevant, since a battery-operated wearable device

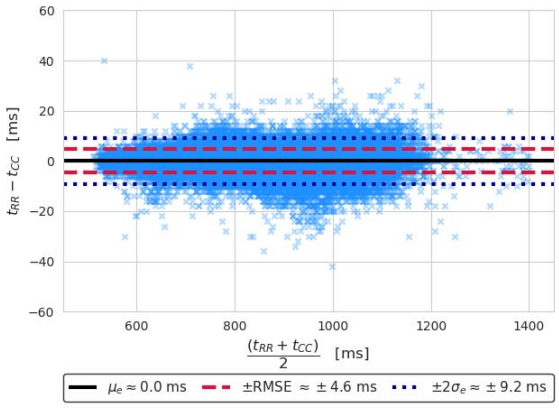

(a)

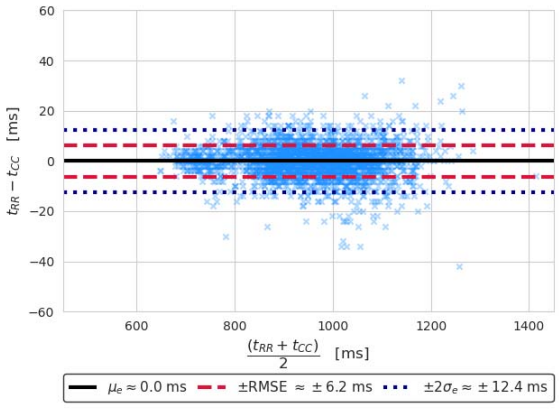

(b)

Fig. 5. Bland–Altman plot of (a) CEBS and (b) custom data sets. Mean, rms, and two times the standard deviation of errors are reported for both data sets.

is envisioned. In order to save battery lifetime, it is important to keep the microcontroller unit (MCU) in low power (sleep) mode for as long as possible, thus limiting the device awakenings. To this purpose, data stream packeting and reduction of sampling frequency are the key assets. In particular, since the SCG signal is known to be band-limited between 1 and 20 Hz [8] and that approximately 50 Hz is sufficient to evaluate kinetic energy in such waveforms [31], it is possible to lower the sampling frequency. However, longer sampling periods may affect the beat-to-beat interval measurement accuracy. In order to explore this possibility, the Custom data set (representing the more challenging scenario, according to the above results) was downsampled to 100 Hz. Only a slight performance impact was found, in absolute terms: the rms error was found to be approximately 7.5 ms; on the other hand, this corresponds to just 0.75 T_s, with almost 97% of errors bounded within ± 1 T_s.

C. Discussion

The present methodology looks forward to the development of a low-cost, wearable device, suitable for multidimensional monitoring and for deployment in practical AAL environments. In this vision, the accelerometer used to sense cardiac activity can be shared to track other relevant

information, related to quantity and quality of movement. For example, a simple classifier can be trained to discriminate epochs with low motion artifacts, like the periods of rest, from moments with more intense motion: the former set can feed SCG analysis, whereas the latter can be used for activity recognition and physical activity assessment purposes. In this article, we hence focus at processing SCG information in relatively quiet setups: in such a condition, the CEBS database can be considered as a reliable benchmark for accuracy, given its controlled setup and long acquisition frames. Since the CEBS database refers to supine position, we extended the investigation scope by accounting for sitting position as well. Low-cost acquisition hardware was designed, and a Custom data set was acquired. The custom setup may more comprehensively account for the AAL use cases.

For the data set consistency's sake, a single (dorsoventral) SCG axis (see Fig. 2) was studied in the custom setup (thus matching the CEBS reference system). The achieved performance metrics improve over our previous work, focused on SCG heartbeat annotation [10]. In particular, average sensitivity is greatly improved, from a previous 91.4% score to the current 98.5% and 99.1% on the CEBS and Custom databases, respectively; standard deviation is also reduced, implying a better stability across subjects: a Mann–Whitney U-test assess significance of such differences ($p < 0.01$). Furthermore, the current results were obtained without leveraging ECG in the calibration phase, therefore truly achieving a fully unsupervised and self-consistent approach, which better suits the target use cases.

Other works used the CEBS database for validation purposes. For example, Choudhary *et al.* [32] explore the feasibility of AO detection by means of wavelet denoising and Shannon energy-based detectors: average 94% and 90% scores are reported for sensitivity and precision, respectively. However, such results were obtained on a subset of 4585 heartbeats, which approximately represent 6.5% of the full records: in this article, instead, no beat was discarded based on quality assessment and the full set was considered. Similarly, Khosrow-Khavar *et al.* [33] report the results of SCG annotation during a lower body negative pressure test in lying position (the monitored): 94% coverage is achieved over approximately 21 600 heartbeats, with an annotation time error of 9 ± 9 ms (mean $\pm$ standard deviation). In a similar setting, Laurin *et al.* [9] compared the detected IM-IM intervals with the reference R-R intervals, achieving an RMSE of 40, 71, 26, 51, and 27 ms for increasing levels of lower body negative pressure; in turn, the average sensitivity in IM detection is 97.2%, 93.0%, 76.9%, 61.6%, and 65.0%, respectively. Moreover, Kaisti *et al.* [34] annotated the heartbeats of the subjects lying on bed for approximately 10 min: by fusing accelerometer and gyroscope information, they achieve high accuracy and precision scores (99.9% and 99.6%, respectively). In this case too, approximately 6.6% of data were discarded in preprocessing, to remove potential artifacts (whereas no temporal segments were discarded in our analysis). Authors also achieved a mean RMSE of 5.6 ms, with a sampling rate of 800 Hz ($\approx 4.5\ T_s$). The results achieved by our proposed methodology are well compared with such works in literature, featuring a lower RMSE error of 4.6 ms (2.3 T_s) for the CEBS data set and for the Custom one, considering the equivalent length in the sampling unit T_s.

IV. Conclusion

This article presents an automated procedure for the precise detection of heart cycles from the SCG signals. The procedure is completely unsupervised: an initial calibration is self-performed, based on the SCG traces only. Heartbeat detection and timing annotation are split in two subtasks. The first one identifies the candidate beat complexes by means of suitably defined detection signals: further refinements are carried out to improve detection sensitivity. The second task performs annotation, by best aligning the SCG candidate beats to a template, extracted during calibration: a cross correlation metric is used to guide such fine alignment. The main algorithm phases and parameters were reviewed, and their impact over performance metrics was independently assessed. Validation was performed on two different data sets, to assess robustness against different acquisition setups (lying subjects in the public CEBS database and sitting subjects in the Custom data set). High sensitivity and precision scores were achieved on both data sets, highlighting good ability to detect as much beats as possible, without incurring in false annotations and without preliminary discarding of low-quality measures. Comparisons of beat-to-beat intervals extracted from SCG against the ECG gold-standard show a very good agreement: R^2 scores of 0.993 and 0.984 were measured on the CEBS and Custom databases; furthermore, an RMSE of approximately 4.7 ms was measured (i.e., two samples), which improves over literature. The present setup looks forward to the development of a wearable device suitable for multidimensional monitoring, with the same accelerometer used for SCG acquisition possibly being exploited for physical-activity tracking tasks as well. This would result in a versatile, inexpensive, and scarcely intrusive device, particularly suitable for long-term monitoring in AAL environments.

References

[1] C. Dobre, C. X. Mavromoustakis, N. M. Garcia, G. Mastorakis, and R. I. Goleva, "Introduction to the AAL and ELE Systems," in *Ambient Assisted Living and Enhanced Living Environments: Principles, Technologies and Control*. Amsterdam, The Netherlands: Elsevier, 2017, pp. 1–16.

[2] B. Andò, S. Baglio, C. O. Lombardo, and V. Marletta, "A multisensor data-fusion approach for ADL and fall classification," *IEEE Trans. Instrum. Meas.*, vol. 65, no. 9, pp. 1960–1967, Sep. 2016.

[3] N. Mora, G. Matrella, and P. Ciampolini, "Cloud-based behavioral monitoring in smart homes," *Sensors*, vol. 18, no. 6, p. 1951, Jun. 2018.

[4] N. Mora *et al.*, "IoT-based home monitoring: Supporting practitioners' assessment by behavioral analysis," *Sensors*, vol. 19, no. 14, p. 3238, Jul. 2019.

[5] H. Al Osman, M. Eid, and A. El Saddik, "A pattern-based windowed impulse rejection filter for nonpathological HRV artifacts correction," *IEEE Trans. Instrum. Meas.*, vol. 64, no. 7, pp. 1944–1957, Jul. 2015.

[6] K. V. Madhav, M. R. Ram, E. H. Krishna, N. R. Komalla, and K. A. Reddy, "Robust extraction of respiratory activity from PPG signals using modified MSPCA," *IEEE Trans. Instrum. Meas.*, vol. 62, no. 5, pp. 1094–1106, May 2013.

[7] D. M. Salerno and J. Zanetti, "Seismocardiography for monitoring changes in left ventricular function during ischemia," *Chest*, vol. 100, no. 4, pp. 991–993, Oct. 1991.

[8] O. T. Inan *et al.*, "Ballistocardiography and seismocardiography: A review of recent advances," *IEEE J. Biomed. Health Inform.*, vol. 19, no. 4, pp. 1414–1427, Jul. 2015.
[9] A. Laurin, F. Khosrow-Khavar, A. P. Blaber, and K. Tavakolian, "Accurate and consistent automatic seismocardiogram annotation without concurrent ECG," *Physiol. Meas.*, vol. 37, no. 9, pp. 1588–1604, Sep. 2016.
[10] N. Mora, F. Cocconcelli, G. Matrella, and P. Ciampolini, "Fully automated annotation of seismocardiogram for noninvasive vital sign measurements," *IEEE Trans. Instrum. Meas.*, to be published.
[11] A. L. Goldberger *et al.*, "PhysioBank, PhysioToolkit, and PhysioNet: Components of a new research resource for complex physiologic signals," *Circulation*, vol. 101, no. 23, pp. e215–e220, Jun. 2000.
[12] A. Taebi, B. Solar, A. Bomar, R. Sandler, and H. Mansy, "Recent Advances in seismocardiography," *Vibration*, vol. 2, no. 1, pp. 64–86, Jan. 2019.
[13] M. Di Rienzo, E. Vaini, and P. Lombardi, "Development of a smart garment for the assessment of cardiac mechanical performance and other vital signs during sleep in microgravity," *Sens. Actuators A, Phys.*, vol. 274, pp. 19–27, May 2018.
[14] M. J. Tadi *et al.*, "Gyrocardiography: A new non-invasive monitoring method for the assessment of cardiac mechanics and the estimation of hemodynamic variables," *Sci. Rep.*, vol. 7, no. 1, p. 6823, 2017.
[15] N. Jeger-Madiot, J. Gateau, M. Fink, and R.-K. Ing, "Non-contact and through-clothing measurement of the heart rate using ultrasound vibrocardiography," *Med. Eng. Phys.*, vol. 50, pp. 96–102, Dec. 2017.
[16] S. Kazemi, A. Ghorbani, H. Amindavar, and D. R. Morgan, "Vital-Sign Extraction Using Bootstrap-Based Generalized Warblet Transform in Heart and Respiration Monitoring Radar System," *IEEE Trans. Instrum. Meas.*, vol. 65, no. 2, pp. 255–263, Feb. 2016.
[17] J. Tu and J. Lin, "Fast acquisition of heart rate in noncontact vital sign radar measurement using time-window-variation technique," *IEEE Trans. Instrum. Meas.*, vol. 65, no. 1, pp. 112–122, Jan. 2016.
[18] G. Cosoli, L. Casacanditella, E. P. Tomasini, and L. Scalise, "The non-contact measure of the heart rate variability by laser Doppler vibrometry: Comparison with electrocardiography," *Meas. Sci. Technol.*, vol. 27, no. 6, Jun. 2016, Art. no. 065701.
[19] L. Scalise, V. Mariani Primiani, P. Russo, A. De Leo, D. Shahu, and G. Cerri, "Wireless sensing for the respiratory activity of human beings: Measurements and wide-band numerical analysis," *Int. J. Antennas Propag.*, vol. 2013, pp. 1–10, 2013.
[20] G. Lu, F. Yang, Y. Tian, X. Jing, and J. Wang, "Contact-free measurement of heart rate variability via a microwave sensor," *Sensors*, vol. 9, no. 12, pp. 9572–9581, Nov. 2009.
[21] M. Villarroel *et al.*, "Continuous non-contact vital sign monitoring in neonatal intensive care unit," *Healthcare Technol. Lett.*, vol. 1, no. 3, pp. 87–91, Sep. 2014.
[22] M. Di Rienzo, E. Vaini, P. Castiglioni, P. Lombardi, P. Meriggi, and F. Rizzo, "A textile-based wearable system for the prolonged assessment of cardiac mechanics in daily life," in *Proc. 36th Annu. Int. Conf. IEEE Eng. Med. Biol. Soc.*, Aug. 2014, pp. 6896–6898.
[23] W.-Y. Lin *et al.*, "Identification of location specific feature points in a cardiac cycle using a novel seismocardiogram spectrum system," *IEEE J. Biomed. Health Inform.*, vol. 22, no. 2, pp. 442–449, Mar. 2018.
[24] M. Di Rienzo *et al.*, "Wearable seismocardiography: Towards a beat-by-beat assessment of cardiac mechanics in ambulant subjects," *Autonomic Neurosci.*, vol. 178, nos. 1–2, pp. 50–59, Nov. 2013.
[25] P. Kumar Jain and A. Kumar Tiwari, "A novel method for suppression of motion artifacts from the seismocardiogram signal," in *Proc. IEEE Int. Conf. Digit. Signal Process. (DSP)*, Oct. 2016, pp. 6–10.
[26] A. Q. Javaid *et al.*, "Quantifying and reducing motion artifacts in wearable seismocardiogram measurements during walking to assess left ventricular health," *IEEE Trans. Biomed. Eng.*, vol. 64, no. 6, pp. 1277–1286, Jun. 2017.
[27] C. Yang and N. Tavassolian, "An independent component analysis approach to motion noise cancelation of Cardio-mechanical signals," *IEEE Trans. Biomed. Eng.*, vol. 66, no. 3, pp. 784–793, Mar. 2019.
[28] C. Yang and N. Tavassolian, "Motion artifact cancellation of seismocardiographic recording from moving subjects," *IEEE Sensors J.*, vol. 16, no. 14, pp. 5702–5708, Jul. 2016.
[29] M. A. García-González, A. Argelagós-Palau, M. Fernández-Chimeno, and J. Ramos-Castro, "A comparison of heartbeat detectors for the seismocardiogram," in *Computing in Cardiology*. IEEE, 2013, pp. 461–464.
[30] J. Pan and W. J. Tompkins, "A real-time QRS detection algorithm," *IEEE Trans. Biomed. Eng.*, vol. BME-32, no. 3, pp. 230–236, Mar. 1985.
[31] A. Hossein *et al.*, "Accurate detection of dobutamine-induced haemodynamic changes by kino-cardiography: A randomised double-blind placebo-controlled validation study," *Sci. Rep.*, vol. 9, no. 1, p. 10479, Dec. 2019.
[32] T. Choudhary, L. N. Sharma, and M. K. Bhuyan, "Automatic detection of aortic valve opening using seismocardiography in healthy individuals," *IEEE J. Biomed. Health Inform.*, vol. 23, no. 3, pp. 1032–1040, May 2019.
[33] F. Khosrow-khavar, K. Tavakolian, and C. Menon, "Moving toward automatic and standalone delineation of seismocardiogram signal," in *Proc. 37th Annu. Int. Conf. IEEE Eng. Med. Biol. Soc. (EMBC)*, Aug. 2015, pp. 7163–7166.
[34] M. Kaisti *et al.*, "Stand-alone heartbeat detection in multidimensional mechanocardiograms," *IEEE Sensors J.*, vol. 19, no. 1, pp. 234–242, Jan. 2019.

Federico Cocconcelli received the M.Sc. degrees *(summa cum laude)* in electronic engineering from the University of Parma, Parma, Italy, in 2015 and 2018, respectively, where he is currently pursuing the Ph.D. degree in information technologies under the supervision of Prof. Paolo Ciampolini.

His current research interests include cardio-mechanical signals, noninvasive technologies for physiological parameters monitoring, sensors for smart living environments, and signal processing techniques.

Niccolò Mora received the degree *(summa cum laude)* in electronic engineering and the European Ph.D. degree (Doctor Europaeus) in information technologies from the University of Parma, Parma, Italy, in 2011 and 2015, respectively.

He currently holds an Associate Researcher position with the Engineering and Architecture Department, University of Parma. His research interests span from Internet of Things (IoT)-enabled sensors development (hardware and software) to bio-signal processing, with a particular focus on continuous monitoring of vital signs and daily life human behavioral patterns. His research activity is partly supported and framed within the ambient assisted living (AAL) Joint Programme and the Horizon2020 Programme.

Guido Matrella received the degree in electronic engineering and the Ph.D. degree in information technology from the University of Parma, Parma, Italy, in 1999 and 2003, respectively.

Since 2007, he has been a Researcher Assistant with the University of Parma. His scientific work is mainly based on the design of digital systems using hardware description language (HDL) descriptions for integrated circuits and field-programmable gate array (FPGAs). In the latest years, his main research activities are framed in the assistive technology field and, in particular, in the use of networks of smart sensors to elderly home behavior monitoring. Within this field, often called ambient/active assisted living (AAL), he participated in several European Projects in the framework of AAL Joint Programme and Horizon2020.

Paolo Ciampolini received the degree *(summa cum laude)* in electronic engineering and the Ph.D. degree in electronics and computer sciences from the University of Bologna, Bologna, Italy, in 1983 and 1989, respectively.

Since 2001, he has been a Full Professor with the University of Parma, Parma, Italy, where he is in charge of electronics fundamentals and digital design courses. From 2001 to 2008, he was the Chairman of the Board of Electronics with the Engineering Faculty, University of Parma. He is currently serving as a Technical/Scientific Coordinator of two projects funded in the framework of ambient assisted living (AAL) Joint Programme. His research activities include physical and numerical modeling of semiconductor devices, design and optimization of solid-state radiation sensors, digital circuit design, and assistive technology devices.